"Mechanistic Insights into Formic Acid Dehydrogenation promoted by Cu-Amino Based Systems"

Andrea Correa[1*], Michele Cascella[2], Nicola Scotti[3], Federica Zaccheria[3], Nicoletta Ravasio[3*] and Rinaldo Psaro[3]

[1] Department of Chemical Sciences, Federico II University of Naples Via Cinthia-Complesso Monte S. Angelo, 80126 Napoli (Italy)

[2] Department of Chemistry, and Centre for Theoretical and Computational Chemistry (CTCC), University of Oslo, Postbox 1033 Blindern, 0315 Oslo, Norway.

[3] CNR- ISTM, via C. Golgi 19, 20133 Milano (Italy)

Authors to whom correspondence should be addressed

HIGHLIGHTS

- Density functional calculations were performed on Cu-amine complexes.
- The influence of the amine on the geometry of the active site was investigated.
- Migration of an H atom from the formate to the metal was found to be a key step.

KEYWORDS

- Density functional calculations
- Formic acid decomposition
- Hydrogen production

ABSTRACT: A computational study on the molecular mechanism of formic acid dehydrogenation in the presence of Cu-amine complex has been carried out in order to shed light on the role of the amine in determining the catalyst activity. The migration of H from the formate ligand to the metal center has been investigated in detail due to its endothermic nature. The relevance of both basicity and steric hindrance of the amine, as well as its binding ability to the metal center, in promoting hydrogen evolution has been confirmed.

Introduction

Decomposition of formic acid (HCOOH) is a key reaction in several processes associated to H_2 storage and green chemistry. For example HCOOH is a byproduct of the transformation of hydroxylmethyl-furfural (HMF) into levulinic acid, a very significant step in the production of fuels from ligno-cellulosic biomasses [1]. The catalytic dehydrogenation of HCOOH may provide hydrogen *in situ*, which is in fact required in the following hydrogenation of levulinic acid to gamma-valerolactone (GVL) [2]. GVL is a valuable platform molecule with potential of producing both renewable fuels and chemicals [3].

Moreover, HCOOH may be used directly as a fuel in direct formic acid fuel cells [4–7] or as a hydrogen carrier [8–10] with a closed carbon cycle for other hydrogenation reactions.

The development of improved technologies for H_2 generation and storage in a safe and reversible manner is an essential prerequisite for allowing its use as fuel. Such advances require both identification of catalysts able to facilitate HCOOH decomposition, and a molecular detailed understanding of their mechanisms.

Compared to H_2, formic acid is liquid and easy to store; moreover, also compared to methanol, itis considered less dangerous.

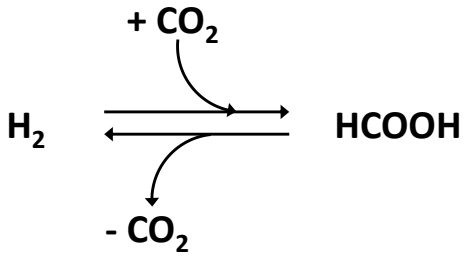

Scheme 1: Formic acid as H_2 carrier

The vapor-phase decomposition of HCOOH has been widely used since the 1960s to test the catalytic properties of various metals and alloys [11-17], as HCOOH is one of the simplest

organic molecules and the simplest carboxylic acid. HCOOH can decompose on metal surfaces through dehydrogenation and/or dehydration processes: dehydrogenation leads to carbon dioxide (CO_2) and hydrogen (H_2) products, while dehydration leads to production of water (H_2O) and carbon monoxide (CO), the latter being a poisoning species for noble metal catalysts such as Pt and Pd. Cu heterogeneous catalysts also have been reported to selectively decompose HCOOH via dehydrogenation to CO_2 and H_2 [18]

Beside heterogeneous catalyst, in the last years a relevant number of papers have been published reporting promising results about HCOOH dehydrogenation by homogeneous catalyst. In particular, interesting results were achieved by rather expensive systems based on noble metal complexes, such as $[RuCl_2(p\text{-cymene})]_2$ or proton-switchable Ir and Rh complexes.[19-22] However, also Fe and Co complexes with PNP pincer ligands have shown to be effective catalysts for HCOOH dehydrogenation in the presence of a base [23-26]

Recently, some of us [27] investigated the reactivity of simple copper complexes (usually a single Cu(II) compound) toward HCOOH decomposition, and reported the results obtained in the production of H_2 from HCOOH/amine adducts. In the absence of copper species such adducts gave no gas evolution; on the contrary, as soon as $Cu(OAc)_2$ was added to the solution, formation of H_2 and CO_2 was observed, yielding in 3 hours a total volume of 20 ml. The use of different copper compounds did not lead to significant differences in the conversion and the total gas volume produced due to the rapid replacement of pristine ligands by amine and $HCOO^-$ (that are present in high concentration in the reaction medium). From these results copper compounds appear as promising catalysts for H_2 production. Moreover, the activity of this catalysts can be finely tuned through the choice of the amine while deactivation (by reduction of Cu(II) to Cu(0)) can be easily controlled. More in depth, a very interesting and evident effect was observed by changing the amine ligands: in particular it has

been observed that by lowering the basicity of the amine the activity decreases. However, the role played by the amine nature appears to be more complex and not linked only to its basicity, $NBut_3$ being more active than NEt_3 although their pK_b is very similar (3.11 vs 2.99). The particular case of ethylenediamine is worth noting: despite its high basicity (pK_b = 3.29) the reaction does not proceed. This behavior clearly underline a coordination effect of the amine on the metal center. Ethylendiamine coordinates to the copper center in a chelate fashion forming a very stable and inactive complex suggesting that some flexibility of the geometric structure of the complex is required to support catalytic activity. Therefore other parameters were taken into account such as the amine nucleophilicity and its steric hindrance, assessed by the cone angle, showing that activity increases by increasing the steric hindrance of the amine ligands and by decreasing nucleophilicity, clearly confirming that the role of amine is not limited to formic acid deprotonation.

Starting from this findings, in this paper we report a computational study on the molecular mechanism of formic acid dehydrogenation by Cu-amine complex and in particular into the coordination geometry of the possible active site.

To better understand the role played by the amine nature on the catalytic activity three different amine ligands have been considered: triethylamine (NEt_3), tributylamine (NBu_3) and diphenylamine ($NHPh_2$), see Scheme 2. Systems containing NEt_3 as the amine are slightly less active than those containing NBu_3 while a strong decrease in the activity is observed in the presence of $NHPh_2$.. So the activity trend of these systems is $NBu_3 > NEt_3 >> NHPh_2$

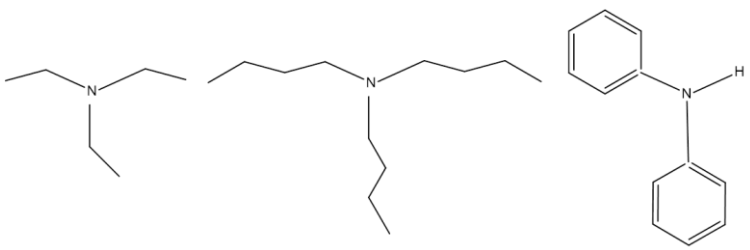

NEt_3 NBu_3 $NHPh_2$

Scheme 2

Computational details.

The electronic structure problem for all the systems investigated was solved by Density Functional Theory, using the hybrid Becke's three parameter exchange functional combined with correlation functional of Lee, Yang and Parr to approximate the exchange and correlation functional in the Kohn-Sham equations.[29,30,31] The Kohn-Sham orbitals were expanded over a 6-31G(d,p) basis set centered over the nuclei of the system.[32,33] All calculations were performed at the standard Gaussian 09 standard settings. [28]

Transition state structures for amine dissociation were localized by performing linear transit evaluation on the Cu-N distances starting from 2.00 Å to 2.60 Å with a Δr of 0.05. The maximum in energy was found for r = 2.50 Å. On these structures, transition state searches were performed and the true nature of transitions states was ensured by frequency calculations. β-H transfer transition states were located by direct optimization from a suitable initial geometry.

All ΔE values reported in Table 1 and Table 2 were calculated as the difference between the energy of products and the energy of reactants, in the relative reactive step.

Buried Volume percentages (%Vbur), defined as the percent of the total volume of an ideal sphere occupied by a ligand, were calculated according with refs 34-35. Specifically, in this approach a sphere of a defined radius R, center at the metal center is defined [34-37]. For our analysis, we used a value of R= 3.5 Å as previously suggested in the literature [36,37]. The volume of this sphere represents the potential coordination sphere space around the metal occupied by a ligand/ligand fragment according to eq.1 and eq. 2 :

$$Vsphere = Vfree + VBur \quad \text{(eq.1)}$$

$$\%VBur = \frac{VBur}{Vsphere} 100$$

(eq 2)

For more details about %Vbur calculation see references 34 and 35.

Results and Discussion

Copper is introduced in the system as Cu(II) compound. During the reaction the catalytic system tends to deactivate with time, producing a discoloring of the solution, that indicates the reduction of Cu(II) to Cu(I), followed by the formation of a red precipitate of metallic Copper (Cu(0)). However, the catalyst can be easily reactivated before complete reduction to the metallic phase by simply opening the reactor to air, which re-oxidizes the Cu(I) species into the most active Cu(II) species.

Following previous experimental and computational studies[26,38,39]on molecular catalyst for HCOOH decomposition, we investigated the mechanism reported in Scheme 3.

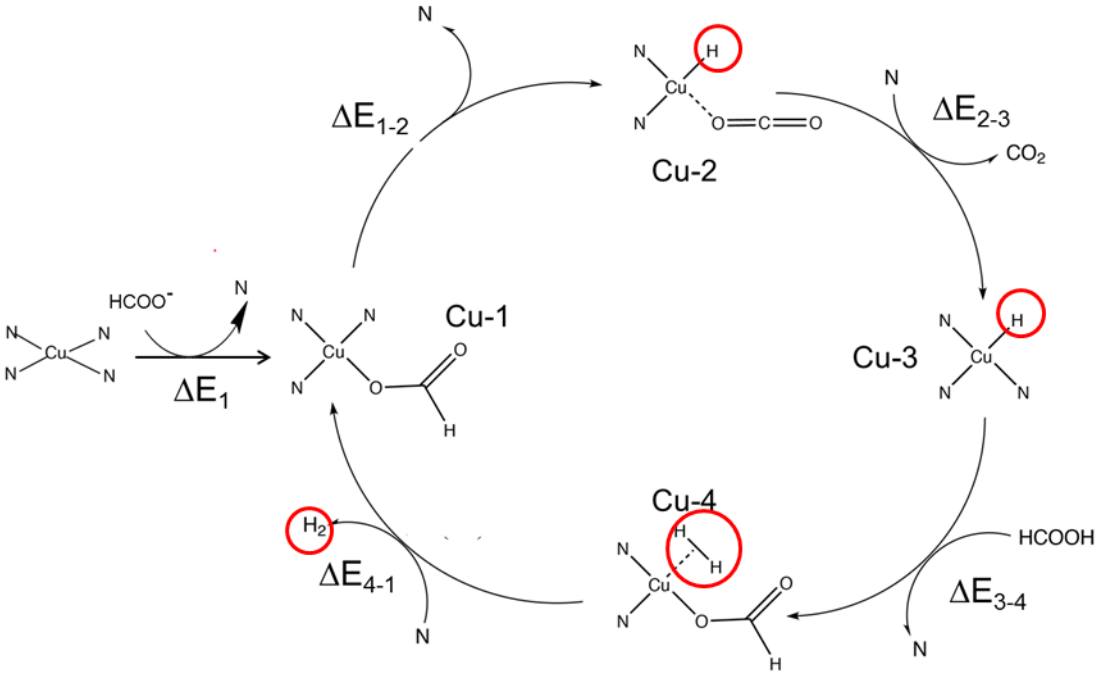

Scheme 3

The first step, in scheme 3, is the formation of a complex between the amino-Cu(II) system and the formate anion (Cu-1, in Scheme 3) by elimination of one amino ligand from the tetra-amino-Cu(II) complex. Subsequent β-hydride elimination leads to intermediate Cu-2. From intermediate 2 CO_2 elimination, assisted by coordination of another amine molecule (that are present in large excess in the reactor) ends up in formation of the Cu-H compound labeled as Cu-3 in Scheme 3. Then coordination of formic acid (Cu-4) followed by hydrogen abstraction restores the starting complex Cu-1.

Table 1 reports the values of ΔE of reaction relative to the formation of Cu(II)-1 intermediate starting from the relative tetra-amino precursors. Figure 1 (top side) shows the optimized structures for the $[Cu(NR_3)_4]^{2+}$ complexes. The calculated Buried volume values for each tretramino-Cu(II) complexes are also reported in Table 1. The buried volume (%Vbur) is defined as the percent of the total volume of a sphere occupied by a ligand, see computational details. %Vbur gives information about the steric hindrance of the amino ligand, i.e. higher %Vbur values means higher steric hindrance.

The volume of this sphere represents the potential coordination sphere space around the metal occupied by a ligand/ligand fragment, see computational details. The calculated buried volume are quite similar for all amino-ligands, the highest value is calculated in the case of NBu_3 ligand.

More in depth, changing of the amino-ligand does not produce any relevant change in the metal-N distances, as well as in the N-Cu-N angles. In all three structures, reported in Figure 1 Cu-N distances stay around 2.18-2.20 Å, and N-Cu-N angles are about 110 degree, indicating a tetrahedral geometry around the metal center.

About the energetic of the reactive steps, sketched in Scheme 3, beside oxidation state II, also oxidation state I of the Cu atom has been evaluated, since presence of Cu(I) compounds is predictable, at least, during the deactivation process.

Table 1. DFT formation energies for in intermediate Cu-1 and calculated buried volume values

Ligand N	ΔE_1 (kcal/mol)	%VBur
NEt_3	-21.2	28.2
NBu_3	-20.4	30.1
$NHPh_2$	-22.7	29.3

Table 2 reports the energy variation for each steps, (see Scheme 3 for labels) ,for the three different amino-compounds.

As general and remarkable results we found that the only endotermic process is the β-hydride elimination from the coordinated formate that leads to Cu-2 complex, more in depth $\Delta E_{1\text{-}2}$ = 8.3 kcal/mol, 6.1 kcal/mol and14.1 kcal/mol for triethylamine, tributylamine and for diphenylamine, respectively. Elimination of CO_2 molecule easily occurs through coordination of an amine ligand (Cu-2 → Cu-3 step, $\Delta E_{2\text{-}3}$) restoring the tetrahedral coordination geometry around the metal center.

The last steps are the coordination of formic acid ($\Delta E_{3\text{-}4}$) followed by H_2 abstraction ($\Delta E_{4\text{-}5}$) that restore the Cu-1 complex.

Reducing the oxidation state of the copper compounds involved in the catalytic cycle of Scheme 3 the overall chemical scenario does not change but stability of intermediate Cu-2 further decreases, (Table 2 bottom side). Moreover, independently from the oxidation state, with the exception of Cu-2 formation, all the other reactions occur with a gain of energy and their stabilities do not seem to have any correlation with the amine nature . However, it is worth underlining that the total energy gap involved in the cycle is in agreement with the higher activity shown by the NBu_3 complex (Table 2, last column).

Table 2. DFT reaction energies the reactive steps displayed in Scheme 3.

Cu(II)					
Ligand N	ΔE_{1-2} (kcal/mol)	ΔE_{2-3} (kcal/mol)	ΔE_{3-4} (kcal/mol)	ΔE_{4-1} (kcal/mol)	ΔE_{tot} (kcal/mol)
NEt_3	8.3	-3.4	-7.1	-2.0	-4.2
NBu_3	6.1	-2.8	-9.6	-2.1	-8.4
$NHPh_2$	14.1	-2.3	-6.3	-2.6	2.9
Cu(I)					
Ligand N	ΔE_{1-2} (kcal/mol)	ΔE_{2-3} (kcal/mol)	ΔE_{3-4} (kcal/mol)	ΔE_{4-1} (kcal/mol)	ΔE_{tot} (kcal/mol)
NEt_3	18.1	-2.5	-8.7	-3.4	3.5
NBu_3	18.6	-1.8	-11.5	-3.1	2.2
$NHPh_2$	21.5	-1.9	-8.6	-2.9	8.1

These finding allow us to speculate that the β-hydride transfer is the key step of Cu catalyzed decomposition of formic acid, so we decided to better investigate this part of the catalytic cycle. Optimized structure of Cu(II)-1 complexes for all three amino-ligands are reported in figure 1 (bottom side). In the case of NEt_3 and NBu_3 the replacement of one amino ligand with the formate ion does not produce any significant difference in the Cu-N distances that stay around 2.20 Å, On the contrary, the N-Cu-N angles change from 109 to 119 degree, while O-Cu-N angles are observed to be about 99 degrees.

For the diphenylamine ligand the Cu-1 complex shows an hydrogen bond between the free oxygen of formate and a close CH group of the amine. This interaction shortens the Cu-N distances (Δr around 0.11 Å, r_{Cu-N} around 2.10 Å), with respect to the tetra-amino complex, instead the N-Cu-N angle stays around typical tetrahedral values, in particular N-Cu-N is

108 degrees. The nature of amino ligands does not produce any variation in the Cu-O distances in all the three Cu-1 complexes, that distance being always ~1.95 Å.

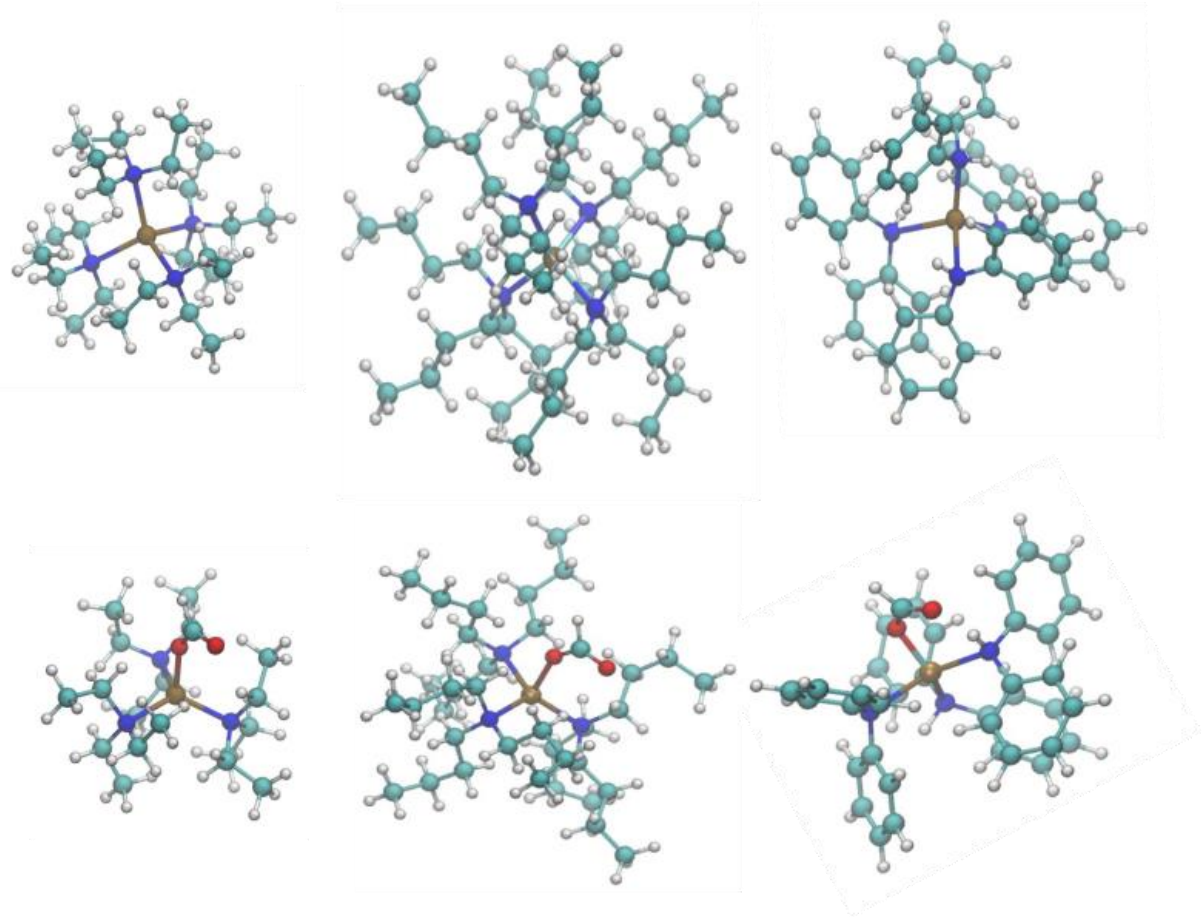

Figure 1 3D minimum structures for the three Cu(II)-1complexes (bottom side) considered in this study and their precursor (top side). Oxygen atoms are reported in red, carbon in ciano, nitrogen in blue, hydrogen white and copper atom is light brown.

Figure 2 reports the optimized structure for the three Cu(II)-2 complexes. Cu-H distances are all about 1.45 Å , in the case of the aliphatic amine the N-Cu-N angles are around 135 degree, while N-Cu-H is around 111 degree. This distortion becomes more evident in the case of the aromatic amine. The Cu-CO_2 distance increases according with the decreasing of Cu-2 stabilities, in particular $r_{Cu\text{-}OCO}$ is 2.41 Å, 2.43 Å and 2.56 Å for NEt_3, NBu_3 and $NHPh_2$ respectively, see Figure 3.

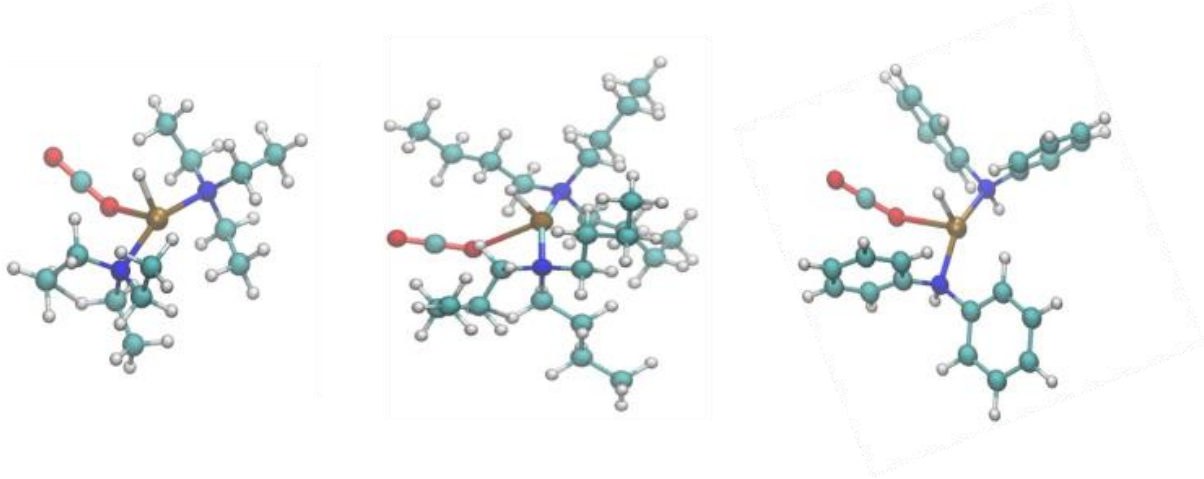

Figure 2. 3D minimum structures for the three Cu(II)-2 complexes considered in this study. Oxygen atoms are reported in red, carbon in ciano, nitrogen in blue, hydrogen white and copper atom is light brown.

The hypothesized mechanism for β-hydride transfer is displayed in Scheme 4. We have considered a dissociative two steps path: the first step is the amine dissociation followed by hydride transfer to the metal center. Figure 4 reports the calculated energy profiles for the three different amino complexes. Since active site are, mainly, Cu(II) complexes, this part of the study has been limited to this oxidation state.

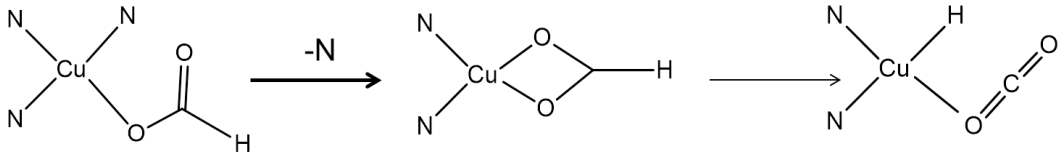

Scheme 4

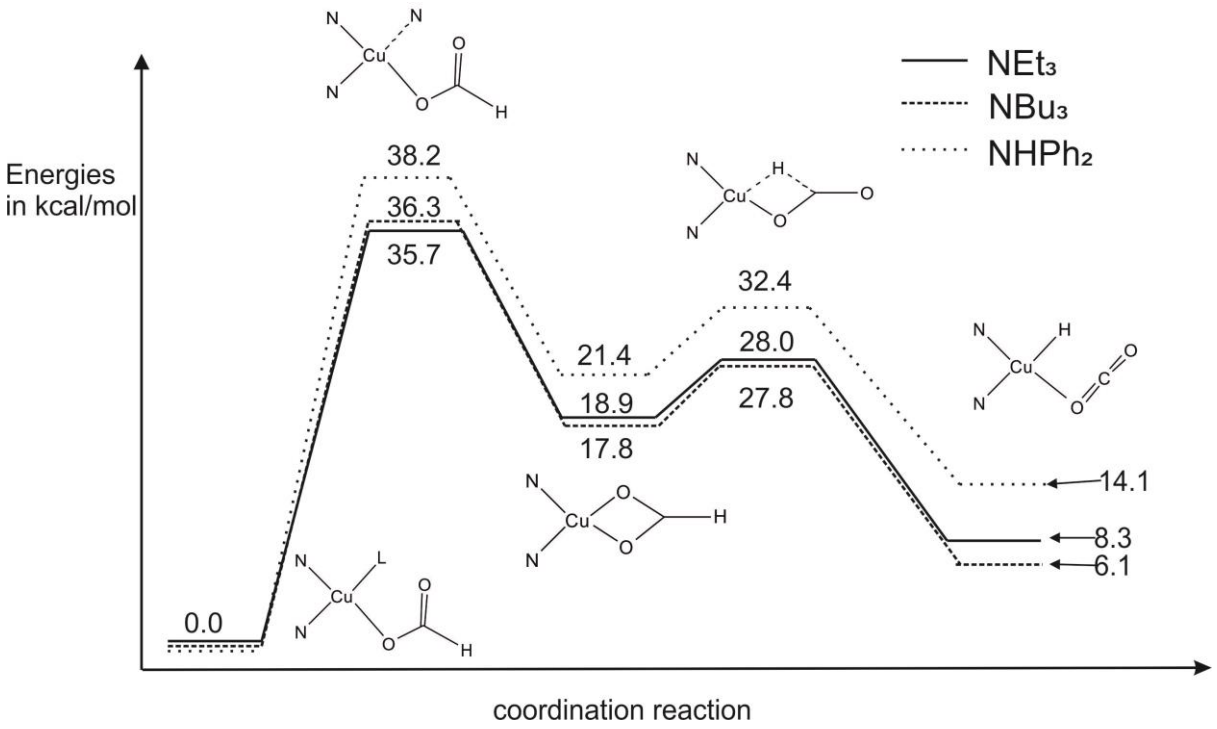

Figure 4. Calculated energy profiles for β-hydride elimination. All energies have been reported in kcal/mol.

Independently from the amine nature, the first step, dissociation of the amine ligand, presents the higher transition state energy (ΔE_{TS1}) that is around 35.7 kcal/mol for triethylamine, 36.3 kcal/mol for tributylamine and 38.2 kcal/mol for diphenylamine. These values indicates a stronger binding ability of $NHPh_2$ to the metal center, with respect to NEt_3 and NBu_3 amine ligand. This is witnessed also by the shorter Cu-N distances found in Cu-1 complex for the $NHPh_2$ ligand with respect to the other two.

The amine dissociation leads to formation of an intermediate structure where both oxygen atoms of formate are interacting with the metal center. Again, no fundamental differences have been found for NEt_3 and NBu_3 ligands. In both case the N-Cu-N and O-Cu-O angles are around 115 and 80 degrees, respectively. Instead, for $NHPh_2$ the two Cu-Oxygen distances are quite asymmetrical, due to the presence of a hydrogen bond between the CH group of one amine ligand and the formate. The β-H transfer occurs with a barrier energy in the range of 28.0 -32.4 kcal/mol. The high barrier energies calculated, for both

steps, are in agreement with the rather high temperature required for the activation of catalytic cycle.

Conclusion

Inspired by the experimental results obtained by some of us, who explored the reactivity of different Cu-amino complexes in formic acid decomposition, we performed a computational study clarifying the mechanistic details of this transformation. Beside the derivation of mechanism the possible effect of different amine on the catalytic cycle has been analyzed. Our calculations indicate that the key step is formation of intermediate 2 . This can occur through a two steps mechanism involving amine dissociation followed by β-hydride transfer from the coordinated formate to the metal center. Both, stability trend of intermediates 2 and transition state barriers are in rather good agreement with the different experimental activity shown by these system [27].

In conclusion, we confirmed the idea firstly proposed by some of us [27] that the effect of the amine ligand is not just related to its basicity. From our calculations we can say that the stabilization of intermediate 2 is the key point in tuning the catalyst activity. Amine basicity, steric properties as well as its binding properties, balance each other in the modulation of intermediate 2 stability, and so in the modulation of catalyst productivity.

Acknowledgments

Italian Ministry for Scientific Research (MIUR) is acknowledged for grant PRIN 2010-2011 PROT 2010A2FSS9_003. This work had the support of the Research Council of Norway (RCN) through the CoE Centre for Theoretical and Computational Chemistry (CTCC) Grant No. 179568/V30 and 171185/V30, and the Norwegian Supercomputing Program (NOTUR), Grant No. NN4654K.

Supporting Information.

Cartesian coordinates of DFT calculated structures are available free of charge in this section.

References

1. D.M. Alonso, J.Q. Bond, J.A. Dumesic, Green Chem., **12** (2010), 1493.

2. J.j. Bozell, G.R. Petersen, Green Chem. **12** (2010), 539.

3. X Alonso, D. M., S.G. Wettstein, J.A. Dumesic, Green Chemistry, **15** (2013), 584.

4. Y. Xingwen, P.G. Pickup, J. Power Sources, **196** (2011), 7951.

5. C. Liu, M. Chen, C. Du, J. Zhang , G. Yin, P. Shi, Y. Sun, Int J Electrochem Sci, **7** (2012), 10592

6. P. Yinghui, Z. Ruiming, S.L. Blair, Electrochem Solid State Lett., **12** (2009), :B23.

7. Y. Xingwen, P.G. Pickup, J Power Sources **182** (2008), 124.

8. A. Boddien, B. Loges, H. Junge, F. Gaertner, J.R. Noyes, M. Beller, Adv Synth Cata., **351** (2009), 2517.

9.C. Fellay, N. Yan, P.J. Dyson , G. Laurenczy, Chem Eur J., **15** (2009), 3752.

10. W. Gan, P.J. Dyson, G. Laurenczy React Kinet Catal Lett., **98** (2009) 205.

11. P. Wang, S. N. Steinmann, G. Fu, C. Michel, P. Sautet, ACS Catal., **7** (2017), 1955.

12. N. Wang, Q. Sun, R.Bai, X. Li, G. Guo, J. Yu, J.Am.Chem.Soc. **138** (2016), 7484.

13. L.A. Larson, J.T. Dickinson, Surf Sci., **84** (1979), 17.

14. F. Solymosi, J. Kiss, I. Kovacs, Surf Sci **192** (1987), 47.

15. S. D. Senanayake, D. R. Mullns, J Phys Chem C, **112** (2008) 9744.

16 M.D. Marcinkowski, J. Liu, C. J. Murphy, M. L. Liriano, N. A. Wasio, F. R. Lucci, M. Flytzani-Stephanopoulos, E. C. H. Sykes, ACS Catal. **7** (2017), 413.

17. L. Wang, J. Zhang, G. Wang G, Zhang W, Wang C, Bian C, Xiao F-S, Chem.Comm. **53** (2017), 2681.

18. Iglesia E, Boudart M . J Catal., **81** (1983), 214.

19. C. Fink, G. Laurenczy, Dalton Transact. **46** (2017) 1670.

20. I. Mellone, F. Bertini, M.Peruzzini, L.Gonsalvi, Catal.Sci.Technol. **6** (2016), 6504.

21. W-H Wang, S. Xu, Y. Manaka, Y. Suna, H. Kambayashi, J. T. Muckerman, E. Fujita, Y. Himeda, ChemSusChem, **7** (2014), 1976.

22. M. Grasemann G. Laurenczy, Energy Environ. Sci., **5** (2012), , 8171.

23. B. Loges, A. Boddien, H. Junge, M. Beller, Angew. Chem. Int. Ed., **47** (2008), 3962.

24. I. Mellone, N. Gorgas, F. Bertini, M.Peruzzini, K. Kirchner, L.Gonsalvi, Organometallics **35** (2016) 3344.

25. H. Ge, J. Yuanyuan, Y. Xinzheng, Inorg. Chem. **55** (2016), 12179.

26. A. Boddien, D. Mellmann, F. Gärtner, R. Jackstell, H. Junge, P. J. Dyson, G. Laurenczy, R. Ludwig, M. Beller, Science, **33** (2011), 1733.

27. N. Scotti, R. Psaro, N. Ravasio and F. Zaccheria RSC Advances **4** (2014), 61514.

28. Gaussian 09, Revision A.02, M. J. Frisch, G. W. Trucks, H. B. Schlegel, G. E. Scuseria, M. A. Robb, J. R. Cheeseman, G. Scalmani, V. Barone, G. A. Petersson, H. Nakatsuji, X. Li, M. Caricato, A. Marenich, J. Bloino, B. G. Janesko, R. Gomperts, B. Mennucci, H. P. Hratchian, J. V. Ortiz, A. F. Izmaylov, J. L. Sonnenberg, D. Williams-Young, F. Ding, F. Lipparini, F. Egidi, J. Goings, B. Peng, A. Petrone, T. Henderson, D. Ranasinghe, V. G. Zakrzewski, J. Gao, N. Rega, G. Zheng, W. Liang, M. Hada, M. Ehara, K. Toyota, R. Fukuda, J. Hasegawa, M. Ishida, T. Nakajima, Y. Honda, O. Kitao, H. Nakai, T. Vreven, K. Throssell, J. A. Montgomery, Jr., J. E. Peralta, F. Ogliaro, M. Bearpark, J. J. Heyd, E. Brothers, K. N. Kudin, V. N. Staroverov, T. Keith, R. Kobayashi, J. Normand, K. Raghavachari, A. Rendell, J. C. Burant, S. S. Iyengar, J. Tomasi, M. Cossi, J. M. Millam, M. Klene, C. Adamo, R. Cammi, J. W. Ochterski, R. L. Martin, K. Morokuma, O. Farkas, J. B. Foresman, and D. J. Fox, Gaussian, Inc., Wallingford CT, 2016.

29. A. D. Becke, J. Chem. Phys., **98** (1993) 5648.

30. C. Lee, W. Yang, and R. G. Parr, *Phys. Rev. B*, **37** (1988) 785.

31. B. Miehlich, A. Savin, H. Stoll, and H. Preuss, *Chem. Phys. Lett.*, **157** (1989) 200.

32. A. D. McLean and G. S. Chandler, J. Chem. Phys., **72** (1980), 5639.

33. K. Raghavachari, J. S. Binkley, R. Seeger, and J. A. Pople, J. Chem. Phys **72** (1980), 650.

34. A. Poater, B. Cosenza, A. Correa, S. Giudice, F. Ragone, V. Scarano, L. Cavallo. Eur. J. Inorg. Chem. (2009), 1759.

35. L. Falivene, R. Credendino, A. Poater, A. Petta, L. Serra, R. Oliva, V. Scarano, L, Cavallo, Organometallics, **35**, (2016), 2286.

36. H. Clavier, A. Correa, L. Cavallo, E. C. Escudero-Adán, J. Benet-Buchholz, A. M. Z. Slawin, S. P. Nolan. Eur. J. Inorg. Chem. (2009), 1767.

37. H. Clavier, S.P. Nolan. Eur. Chem. Commun. **46** (2010), 841.

38. J. H. Barnard, C. Wang, N. G. Berry, J. Xiao, J Chem. Sci., **4** (2013), 1234.

39. J. Li, J. Li, D. Zhang, C. Liu, ACS Catalysis, **6** (2016), 4746.